Int. J. Electrochem. Sci., 13 **(2018)** 8854 – 8866, doi: 10.20964/2018.09.03

International Journal of ELECTROCHEMICAL SCIENCE
www.electrochemsci.org

Silver Nanoparticle Modified Graphene Paste Electrode for the Electrochemical Detection of Lead, Cadmium and Copper

Shirley Palisoc[1,2], *Eldrin T. Lee*[1], *Michelle Natividad**[1,2] *and Lotis Racines*[1,3]

[1] Condensed Matter Research Laboratory, Physics Department, De La Salle University
[2] Condensed Matter Research Unit, CENSER, De La Salle University
2401 Taft Avenue, Manila, Philippines, 922
[3]Central Mindanao University, Maramag, Bukidnon, Philippines, 8714
*E-mail: michelle.natividad@dlsu.edu.ph

Received: 23 March 2018 / *Accepted:* 30 June 2018 / *Published:* 5 August 2018

Silver nanoparticle (AgNP) graphene paste electrodes were fabricated from graphene powder mixed with mineral oil and silver nanoparticles. Anodic stripping voltammetry (ASV) was utilized to simultaneously detect lead (Pb^{2+}), cadmium (Cd^{2+}) and copper (Cu^{2+}). The optimized amounts of mineral oil and AgNP were 80μL and 2mg respectively. The calibration curve of the optimized electrode showed a strong line correlation between the heavy metal concentration and the reduction current for Pb^{2+}, Cd^{2+}, and Cu^{2+}. In addition, the limit of detection is 17 parts per billion (ppb) for Cd^{2+}, 12 ppb for Pb^{2+} and 44 ppb for Cu^{2+}. The optimized electrode was tested on three commercial brands of Puerh tea. Copper metal ions, Cu^{2+}, were found in the tea samples. Lastly, atomic absorption spectroscopy was used to verify the results obtained from ASV.

Keywords: Silver nanoparticle, graphene paste electrode, anodic stripping voltammetry, heavy metals

1. INTRODUCTION

The release of toxic heavy metals in increasingly large quantities to the environment is a great threat to humankind. Heavy metals do not decompose at all; therefore, they continuously accumulate in soil and in human bodies [1]. Among the different pollutants encountered in the environment, heavy metals are a major concern worldwide; cadmium (Cd), lead (Pb) and Copper (Cu) widely proliferate, particularly in wastes deposited in discharges. Due to their cumulative properties and long biological half-life, such exposure to these heavy metals may cause adverse health effects. Metal toxicity could be direct or indirect as in inducing the production of reactive oxygen species that could cause damage to cell macromolecules, notably polyunsaturated lipids and proteins [2]. One of the primary goals of the World Health Organization (WHO) is to be able to monitor the intake of heavy metals of humans

and animals. The threshold set by WHO for cadmium in plants is 20 ppb, that for lead is 2 ppm, and that for copper is 10ppm [3].

There are various techniques used for the detection of heavy metals which includes, colorimetric analysis, UV-vis spectrometry, surface enhanced Raman spectrometry (SERS), atomic fluorescence spectrometry, ion chromatography, inductively coupled plasma mass spectrometry (ICP-MS) and inductively coupled plasma optical emission spectrometry (ICP-OES). However, these methods have drawbacks such as high cost, demand for complex instrumentation and unsuitability for on-field analysis, on top of their being time-consuming. Anodic stripping voltammetry (ASV) has been regarded as an effective technique for the determination of trace metal ions due to an effective preconcentration step followed by electrochemical stripping measurements of the accumulated analytes. Using chemically modified electrode via stripping analysis has shown significant selectivity toward some metal ions. The success of the stripping operation relies on the choice of the working electrode [4].

Electrochemical methods have been developed for the detection and determination of Cd^{2+} and Pb^{2+} [5-12] because these approaches typically do not require expensive equipment. They also provide high specificity and sensitivity while retaining their simplicity [13]. In electrochemical studies, carbon paste electrodes (CPEs) are widely used because of their low background current (compared to solid graphite or noble metal electrodes), low cost, feasibility to incorporate different substances during the paste preparation, easy preparation, simple renewal of their surface and possibilities of miniaturization. Also, the use of CPE eliminates the problem of intermetallic species interference, which often occurs when using a mercury electrode [14]. Carbon paste electrode construction has a variety of methods that employ several types of carbonaceous materials such as graphite, graphene, acetylene black, diamond, carbon nanofibers, carbon microspheres and carbon nanotubes [15-20].

The CPE was originally designed as an alternative to the dropping mercury electrode. The material with paste-like consistency could be used in the voltammetric analysis even though the concept of a dynamic renewable electrode surface was not successful. In previous studies [21, 22], a CPE was modified by placing an electrochemically active surface onto the CPE. Another study [23] investigated the first application for electrosynthesis, which eventually evolved into carbon paste electrodes construction [24, 25]. Kalcher [26] discussed Baldwin's method of directly mixing a solid modifier to the paste. The necessary conditions for a pasting liquid are its practical insolubility in the solution under measurement, a low vapor pressure to optimize both mechanical stability and long lifetime, and the pasting liquid's electrochemical inactivity for voltammetric and amperometric applications measurements. Modifications of carbon paste are done to obtain new sensors with desired, often predefined properties, in contrast to the relatively complicated modifications of solid substrates as mentioned in a previous study [27]. A graphene paste electrode was developed by Parvin [28] for the detection of chlorpromazine. The graphene paste electrode was prepared by mixing 0.5g graphene powder with 180μL mineral oil and was eventually packed into a piston-driven holder about 3mm in diameter. Graphene was utilized for the electrode construction due to its good conductivity.

In this study, a novel silver nanoparticle modified graphene paste electrode (AuNP/GPE) was fabricated, optimized, and used to detect heavy metals in commercial tea samples.

2. METHODOLOGY

2.1. Chemicals, reagents, and real samples

Graphene nanopowder (multilayer graphene; average flake thickness: 60 nm) was purchased from Graphene Supermarket (Calverton, NY, USA). Silver nanopowder (<100 nm particle size), sodium chloride, lead chloride, cadmium chloride, copper chloride, mineral oil, and nitric acid were purchased from Sigma, Aldrich (Sigma-Aldrich Pte Ltd, Singapore). Several brands of Puerh tea samples were used for real sample analysis.

2.2. Glassware and equipment

The following are the equipment used in this study: BOSCH SAE200 electronic balance, BANDELIN SONOREX sonicator bath, BST8 potentiostat/galvanostat, Transferette® micropipette, agate mortar and pestle, AA-6300 Shimadzu atomic absorption spectrophotometer, spatula, crucible, Thermolyne 48000 furnace, La Germania general heat hot plate and glassware such as beakers, petri dish, and graduated cylinder.

2.3. Fabrication of Silver Nanoparticle Modified Graphene Paste Electrode (AgNP/GPE)

The graphene paste mixture was prepared by manually mixing mineral oil, graphene powder and AgNPs for about 25 min using an agate mortar and pestle. The mineral oil served as the binder for the graphene powder for the electrode. The mixture was then packed into a piston-driven electrode holder which was a Teflon syringe with a diameter of 3mm. The tip of the GPE was cleaned with wet filter paper and copper wire was connected to the electrode with a silver paste for the ohmic contact. The length of the GPE was maintained and the amount of graphene was held constant.

2.4. Optimization of Mineral oil and AgNP content

To determine the best electrode, the mineral oil and AgNP content in the electrode were optimized. The amount of mineral oil was varied at 22.5µL, 45µL, 75µL, 90µL, 120µL and 180µL and the AgNP content was varied from 0 to 3mg in 0.5mg increments while holding graphene at 0.21g. The fabricated modified GPEs were then used to detect 10ppm each of Cd^{2+}, Pb^{2+}, and Cu^{2+}.

2.5. Anodic stripping voltammetry (ASV)

A BST8 potentiostat/galvanostat was used for the ASV measurements. The fabricated electrode (working electrode) was placed in the voltammetric cell together with the saturated calomel electrode (reference electrode) and the platinum coil (counter electrode). The electrolyte solution consisted of 0.5844g sodium chloride and 100mL of deionized water. Ten parts per million (10 ppm) each of lead,

cadmium, and copper were used for the optimization of the electrodes; 0.111ppb to 0.745ppm of Pb^{2+} and from 0.183.96 to 0.613ppm of Cd^{2+} were utilized to obtain the calibration curves. Lead and cadmium were detected simultaneously, while copper was detected sequentially. A potential of -0.95V was applied and the deposition time was set at 60s.

2.6. Atomic absorption spectrometry (AAS)

Atomic absorption spectrometry was used to verify the results of ASV. The device used was AA-6300 Shimadzu Atomic Absorption Spectrophotometer. The AAS has a nozzle, this was initially submerged in distilled water to clean it from impurities and then the bottles of the stock solutions were tested. The device was fed with distilled water to ensure cleanliness of the nozzle after testing a solution. After the stock solutions were tested a calibration curve was obtained. The real sample solutions were then compared to the generated calibration curve.

3. RESULTS AND DISCUSSION

3.1. Optimization of Mineral oil and AgNP content

To be able to determine the best electrode, the mineral oil amount was varied while the mass of the graphene was held constant at 0.21g. The mineral oil was varied at 22.5μL, 45μL, 75μL, 80μL, 90μL, 120μL, 180μL, and the resulting electrodes were used to detect Cd^{+2} and Pb^{+2}. As shown by the voltammograms in Fig .1, 80μL gave the highest anodic peak current for both Cd^{2+} and Pb^{2+}. This indicates that 80 μL is the right mineral oil content of the electrode. Increasing the mineral oil content further increased the resistivity of the electrode resulting in a decrease in the anodic peak current [29]. Thus, 80μL was chosen as the optimum amount of mineral oil.

To optimize the AgNP content, 7 electrodes were prepared with varying amounts of AgNP, from 0.5mg to 3mg in 0.5- mg increments, while the mass of the graphene of 0.21g and the mineral oil content of 80μL were held constant. The electrodes were used to detect 10 ppm each of Cd^{2+}, Pb^{2+}, and Cu^{2+}. From the voltammograms for Cd^{2+} and Pb^{2+} (Fig. 2), the electrode with 2mg AgNP attained the highest anodic peak current for both Cd^{2+} and Pb^{2+}. The voltammograms obtained for Cu^{2+} (Fig. 3) also shows that 2mg AgNP produced the highest anodic peak current. This can be attributed to the increase in the electrical conductivity and the rate of electron transfer [30] of the electrode as the amount of AgNP was increased. However, increasing the AgNP content higher than 2mg did not further enhance the current signal. Thus, 2mg was chosen as the optimized amount of AgNP.

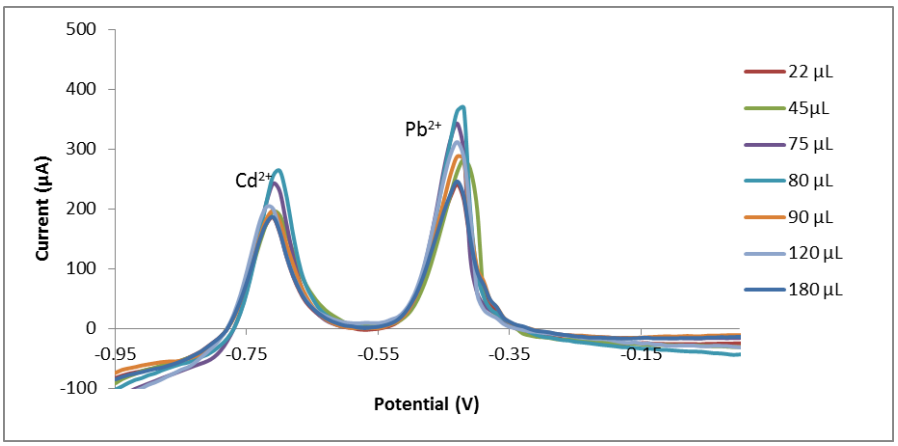

Figure 1. Anodic stripping voltammograms obtained for varying mineral oil content. Supporting electrolyte: 0.1M NaCl solution, 10ppm Pb(II), 10ppm Cd(II). ASV parameters: scan rate = 100 mV/s, accumulation potential = -0.95 V, accumulation time = 60 s, and deposition time = 30 seconds.

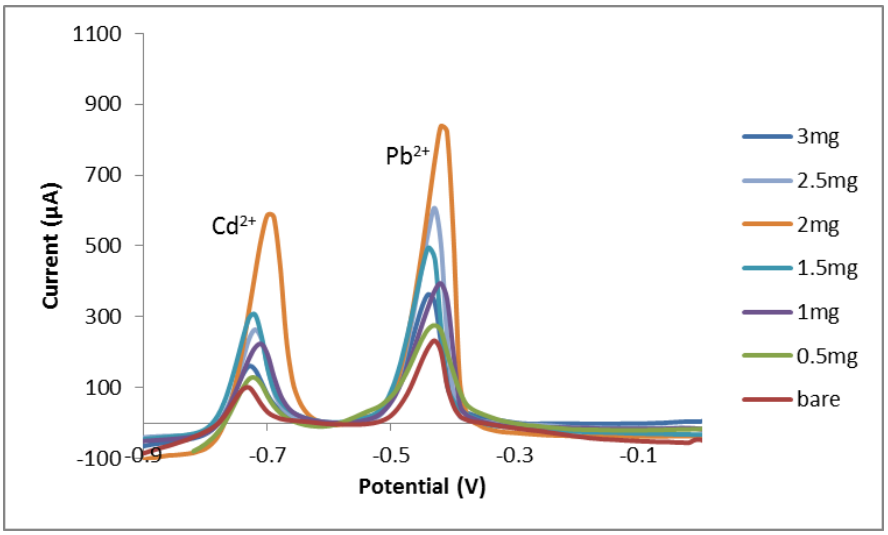

Figure 2. Anodic Stripping Voltammograms of Cd^{2+} and Pb^{2+} with varying AgNP content. Supporting electrolyte: 0.1M NaCl solution, 10ppm Pb(II), 10ppm Cd(II). ASV parameters: scan rate = 100 mV/s, accumulation potential = -0.95 V, accumulation time = 60 s, and deposition time = 30 seconds.

From the mineral oil and AgNP optimization, the electrode with a mineral content of 80µL and AgNP content of 2mg was chosen as the best electrode. Figure 4 shows the anodic stripping voltammograms obtained with the optimized AgNP/GPE and a bare GPE. It can be observed from the said figure that the anodic peak currents for Cd^{2+}, Pb^{2+}, and Cu^{2+} were greatly enhanced due to the modification of GPE by AgNP. Among all metals, silver is the most electrically conductive. Also, it has been identified as a highly active electrocatalyst in alkaline solutions for the oxidation of small organic molecules, due to the formation of reactive adsorbed OH species that influence the kinetics of the reaction [31].

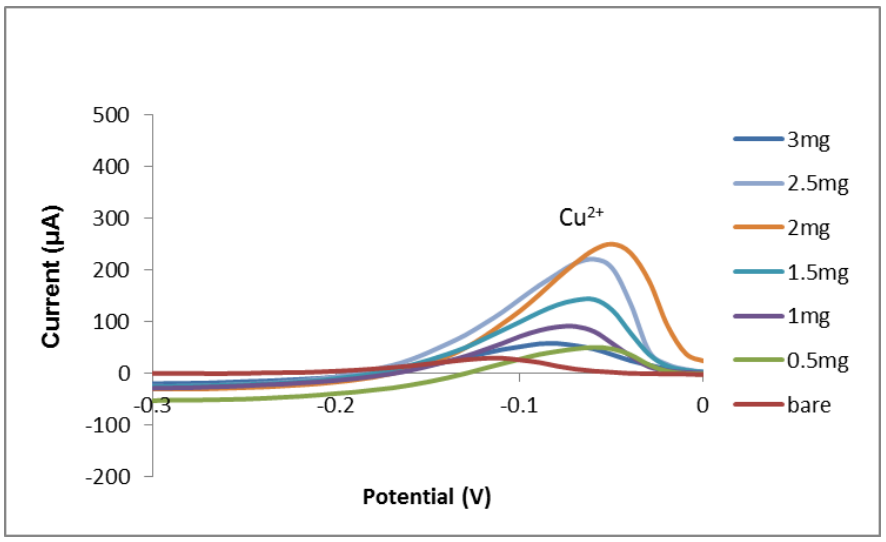

Figure 3. Anodic Stripping Voltammograms of Cu^{2+} with varying AgNP content. Supporting electrolyte: 0.1M NaCl solution, 10ppm Cu(II). ASV parameters: scan rate = 100 mV/s, accumulation potential = -0.95 V, accumulation time = 60 s, and deposition time = 30 seconds.

In related studies, nanosized Ag has been demonstrated to act as an effective sensing material for the detection of pesticides [32] and toxic substances such as lead [33] as well as important species such as hydrogen peroxide and hydrazine [34-36].

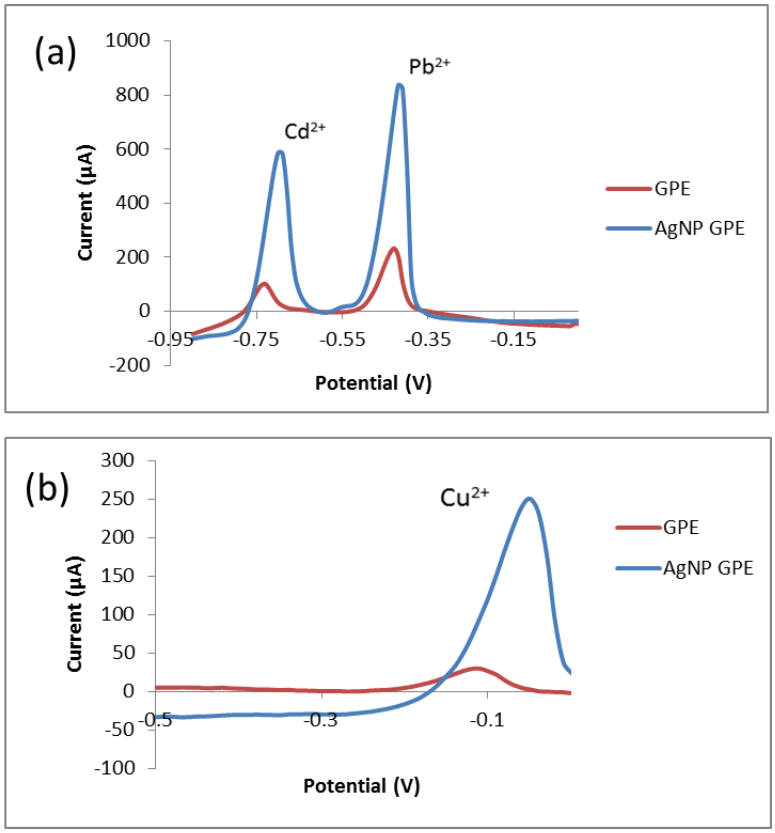

Figure 4. (a) ASV voltammograms of Cd^{2+} and Pb^{2+} with bare GPE and AgNP modified GPE. (b) ASV voltammograms of Cu^{2+} with bare GPE and AgNP modified GPE.

Thus, the increase in the peak currents of Cd^{2+}, Pb^{2+}, and Cu^{2+} can be attributed to the increase in the electrical conductivity of the electrode due to the addition of AgNP. The combined high surface-to-volume ratio of graphene and the high conductivity of AgNP made the electrode more sensitive in detecting the heavy metals.

3.2. ASV Parameter Optimization

To obtain the highest peak current for the best electrode, the accumulation potential and accumulation time were optimized as well. The optimized electrode was used to detect 10ppm each of Cd^{2+}, Pb^{2+}, and Cu^{2+} in the electrolyte solution.

3.3. Accumulation potential

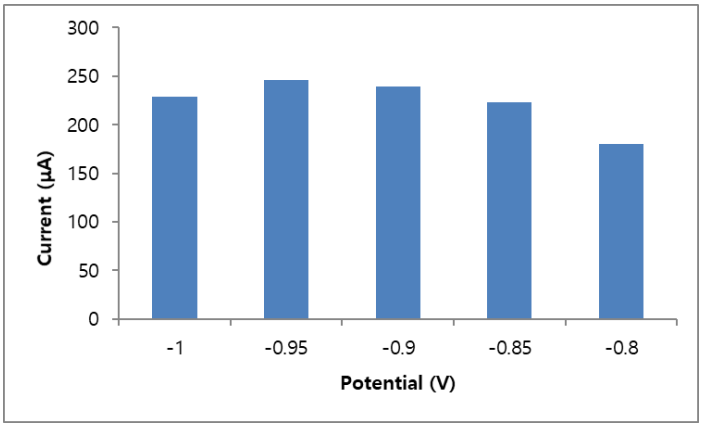

Figure 5. Peak currents for different accumulation potential for Cd^{2+}. Supporting electrolyte: 0.1M NaCl solution with 10ppm Cd(II) and 10ppm Pb(II). ASV parameters: scan rate = 100 mV/s, accumulation time = 60 s, and deposition time = 30 seconds.

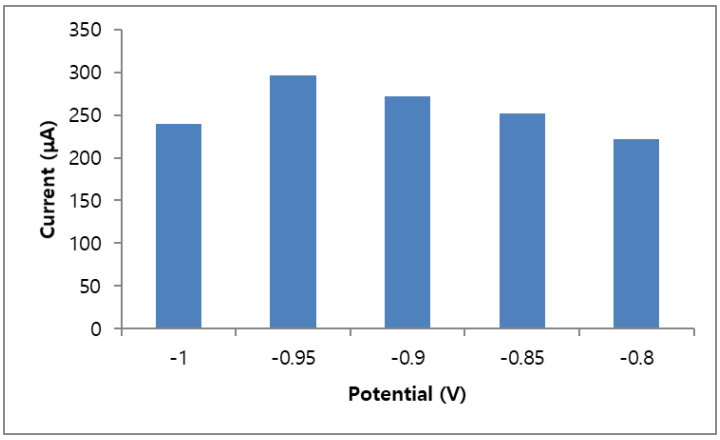

Figure 6. Peak currents for different accumulation potential for Pb^{2+}. Supporting electrolyte: 0.1M NaCl solution with 10ppm Pb(II) and 10ppm Cd(II). . ASV parameters: scan rate = 100 mV/s, accumulation time = 60 s, and deposition time = 30 seconds.

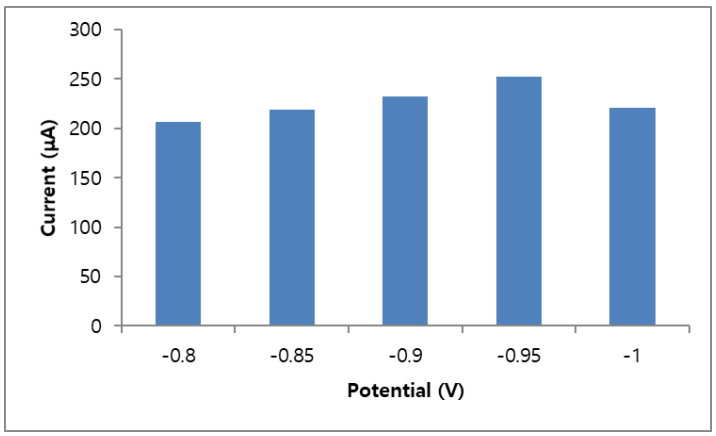

Figure 7. Peak currents for different accumulation potential for Cu^{2+}. Supporting electrolyte: 0.1M NaCl solution with 10ppm Cu(II). ASV parameters: scan rate = 100 mV/s, accumulation time = 60 s, and deposition time = 30 seconds.

The accumulation potential was varied from -0.8V to -1.0V with -0.5V intervals. The accumulation and deposition times were set to a constant value of 30s. As seen in Fig. 5 to 7, the highest peak current was obtained at an accumulation potential of -0.95V for Cd^{2+}, Pb^{2+}, and Cu^{2+}. This can be attributed to the fact that at this accumulation potential, Cd^{2+}, Pb^{2+}, and Cu^{2+} are reduced more efficiently [37].

3.4. Accumulation time

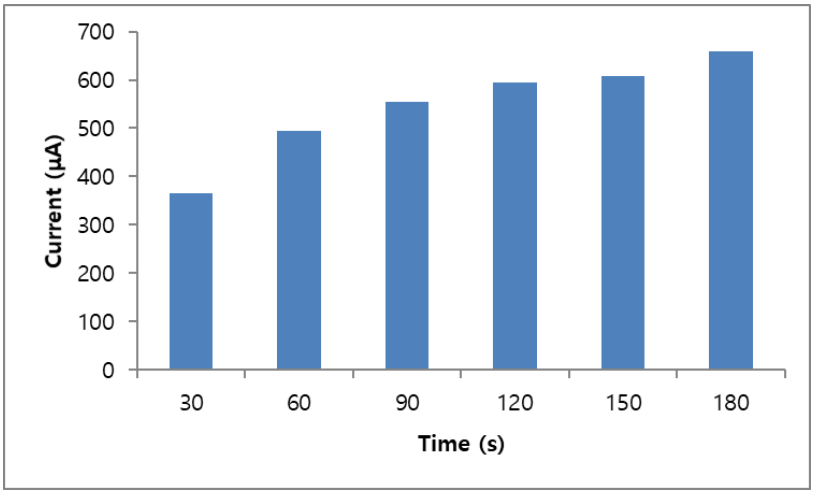

Figure 8. Peak currents for different accumulation time for Cd^{2+}. Supporting electrolyte: 0.1M NaCl solution with 10ppm Cd(II) and 10ppm Pb(II). ASV parameters: scan rate = 100 mV/s, accumulation potential = -0.95 V, and deposition time = 30 s.

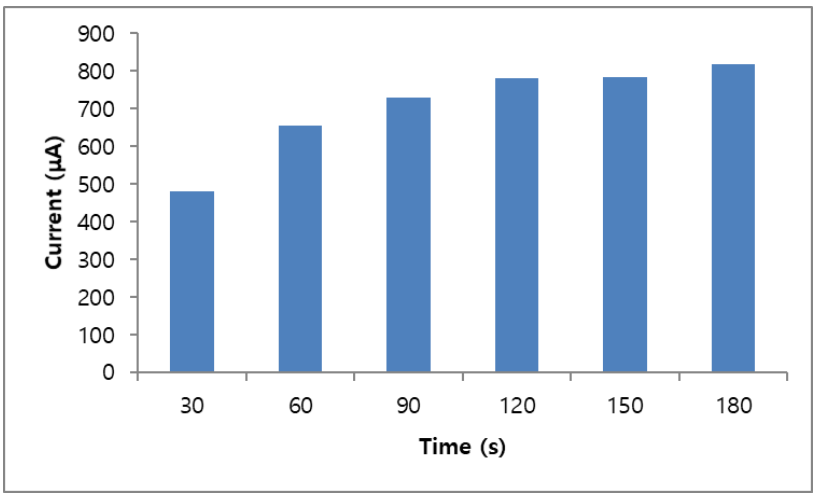

Figure 9. Peak currents for different accumulation time for Pb^{2+}. Supporting electrolyte: 0.1M NaCl solution with 10ppm Cd(II) and 10ppm Pb(II). ASV parameters: scan rate = 100 mV/s, accumulation potential = -0.95 V, and deposition time = 30 s.

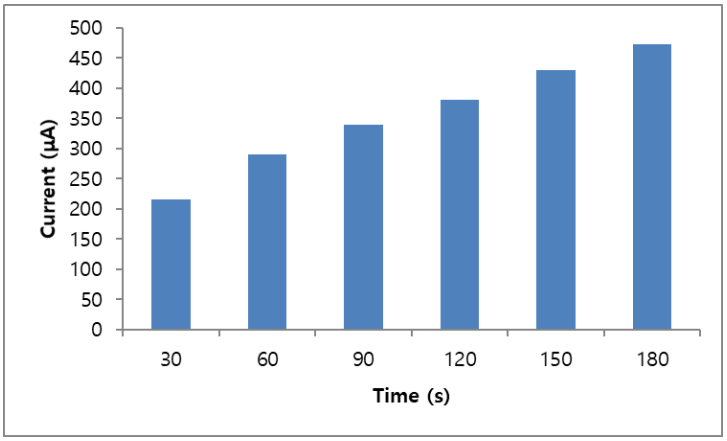

Figure 10. Peak currents for different accumulation time for Cu^{2+}. Supporting electrolyte: 0.1M NaCl solution with 10ppm Cu(II). ASV parameters: scan rate = 100 mV/s, accumulation potential = -0.95 V, and deposition time = 30 s.

The accumulation time was varied from 30s to 180s with 3s intervals. An accumulation potential of -0.95V was applied to enable the metal ions to adsorb on the surface of the working electrode, with a constant deposition time of 30s. It can be seen in Figs. 8 to 10 that the peak current increased linearly along with the accumulation time; however, in order to maintain the time efficiency of the electrode, 60s was used in further runs.

3.5. Calibration Curves

The calibration curves of the optimized electrode were obtained by varying the concentrations of Cd^{2+} and Pb^{2+} from 111.765 ppb to 745.1 ppb for Pb^{2+} and from 183.96 ppb to 613.2 ppb for Cd^{2+}. Cu^{2+} concentration was varied from 94.54 ppb to 945.4 ppb. Figure 11 shows the voltammograms and the calibration curves for Cd^{2+} and Pb^{2+}. There is a strong line correlation between the heavy metal concentration and the reduction current indicating that more heavy metals accumulate on the electrode

surface as the heavy metal concentration was increased. This result was also observed in previous studies [5,6,7]. The same trend was obtained for Cu^{2+} as seen in Fig. 12.

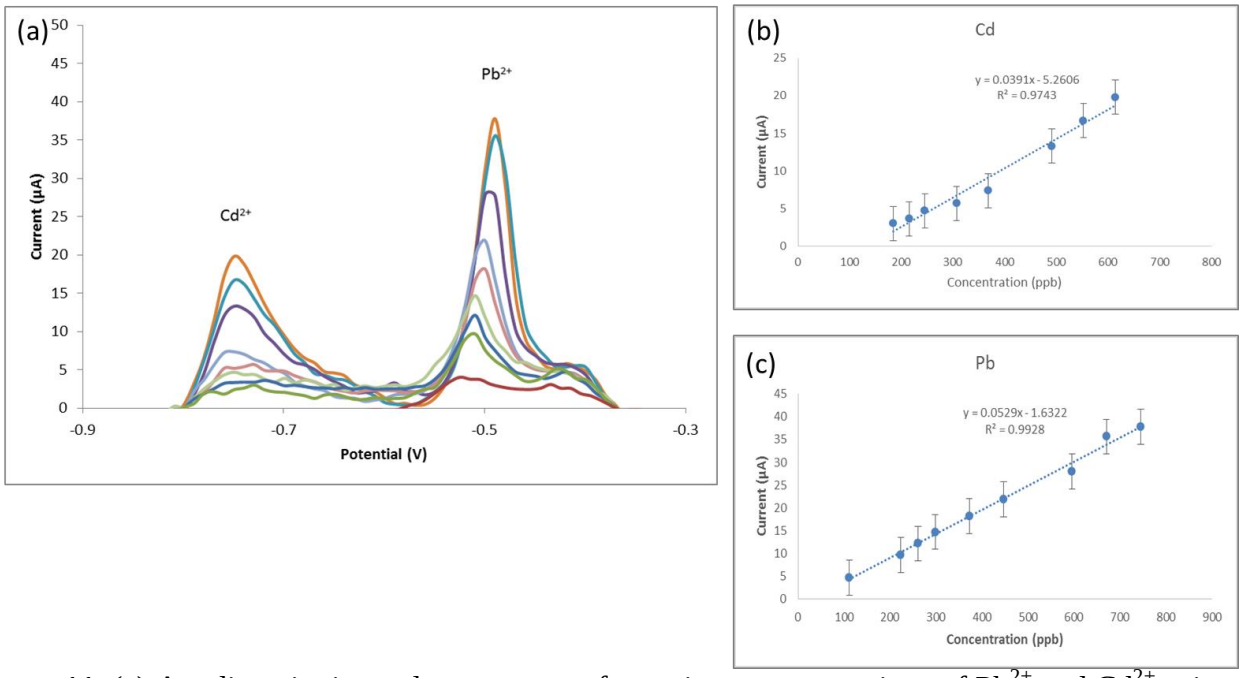

Figure 11. (a) Anodic stripping voltammograms for various concentrations of Pb^{2+} and Cd^{2+} using the optimized GPE. (b) Calibration curve for Cd^{2+}. (c) Calibration curve for Pb^{2+}. Supporting electrolyte: 0.1M NaCl solution. ASV parameters: scan rate = 100 mV/s, initial potential = -0.9 V, deposition time = 60 s, and rest period = 30 seconds.

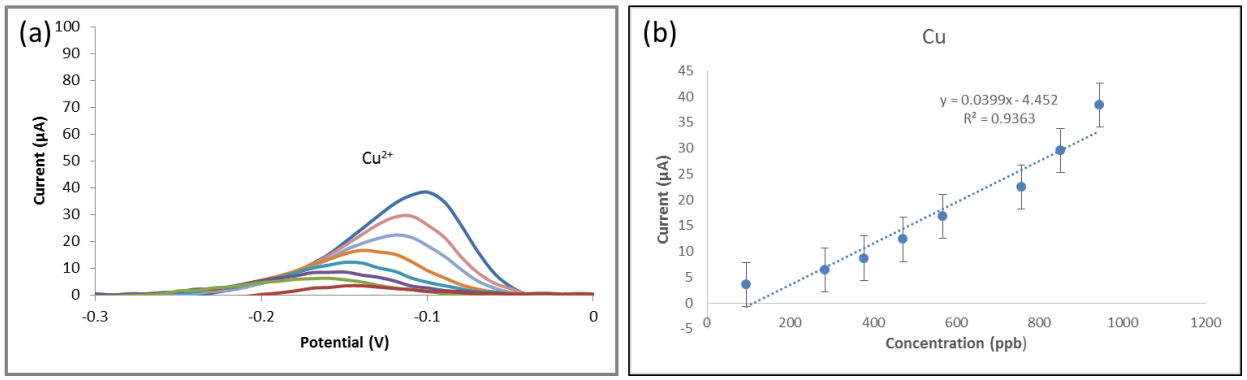

Figure 12. (a) Anodic stripping voltammograms for various concentrations of Cu^{2+} detected using the optimized GPE. (b) Calibration curve for Cu^{2+}. Supporting electrolyte: 0.1M NaCl solution. ASV parameters: scan rate = 100 mV/s, initial potential = -0.9 V, deposition time = 60 s, and rest period = 30 seconds.

3.6. Limit of Detection and Limit of Quantitation

The limit of detection (LOD) and limit of quantification (LOQ) were calculated using the calibration curves and are shown in Table 1. The performance comparison of the fabricated electrode

with previous works is shown in Table 2. It can be observed from the table that the fabricated electrode in this study has a lower LOD than most of the electrodes reported previously.

Table 1. Limit of Detection and Limit of Quantitation

	LOD	**LOQ**
Cd^{2+}	17 ppb	51 ppb
Pb^{2+}	12 ppb	36 ppb
Cu^{2+}	44 ppb	133 ppb

Table 2. Performance comparison of the modified electrode with previous works.

Electrode	Modifier	Method	Detection Limit	Reference
Indium Tin Oxide	$[Ru(NH_3)_6]^{3+}$/Nafion	ASV	Pb & Cd - 500 ppb	[5]
Glassy Carbon	AuNP/$[Ru(NH_3)_6]^{3+}$/Nafion	ASV	Pb - 45 ppb Cd - 200 ppb	[10]
Glassy Carbon	Chitosan/carbon nanotubes	SWASV	Pb - 600 ppb Cd - 800 ppb Cu – 100 ppb	[38]
Glassy carbon	$[Ru(bpy)_3]^{2+}$/graphene/ Nafion	DPV	Pb - 48 ppb Cd - 49 ppb Cu – 28 ppb	[39]
Carbon Paste	Coconut Shell powder	ASV	Cd – 105 ppb	[40]
Graphene Paste	Silver Nanoparticles	ASV	Cd - 17 ppb Pb - 12 ppb Cu – 44 ppb	This work

3.7. Real Sample Analysis

Three brands of Puerh tea were tested: (1) Brand A, (2) Brand B, and (3) Brand C. Three batches of each brand were prepared. The tea leaves of mass 1g were ground to powder form using an agate mortar and pestle, then placed in a ceramic crucible. The sample was carbonized on a hot plate and then dry ashed in a furnace at 500 °C. The sample was then mixed with 5mL of nitric acid and was placed on a hot plate to completely dry the mixture. Finally, it was dissolved in the electrolyte solution and then subjected to ASV and AAS for trace metal analysis.

Table 3 shows the ASV and AAS results of the real sample analysis. Both ASV and AAS detected Cd^{2+}, Pb^{2+}, and Cu^{2+} in the real samples. As can be seen from the table, the concentrations detected via ASV for Cd^{2+} and Cu^{2+} are closer to the values detected by AAS than those for the Pb^{2+}. This may be attributed to the non-homogeneity of the assay when the measurements were taken. According to the World Health Organization, the threshold is 20 ppb for cadmium, 2 ppm for lead, and 10ppm for copper [3]. It can be observed from the table that the lead and copper contents of the samples are below the WHO limit. However, the cadmium content exceeds the WHO limit. Thus, the tea samples can be considered to be toxic.

Table 3. Anodic Stripping Voltammetry vs Atomic Absorption Spectrometry.

	Cd^{2+}		Pb^{2+}		Cu^{2+}	
Tea samples	ASV (ppm)	AAS (ppm)	ASV (ppm)	AAS (ppm)	ASV (ppm)	AAS (ppm)
Brand A	1.18	0.95	0.48	0.17	1.88	2.06
Brand B	1.18	1.33	0.17	0.85	2.05	2.17
Brand C	2.83	0.99	0.13	1.13	1.50	1.62

4. CONCLUSION

The fabrication of the improvised AgNP-modified GPE was proven effective in detecting lead, cadmium, and copper. The AgNP-modified GPE was remarkable in terms of its significant LOD of 17 ppb for Cd^{2+}, 12 ppb for Pb^{2+} and 44 ppb for Cu^{2+} despite its improvisation. The AgNP, having excellent conductivity, greatly enhanced the sensitivity of the GPE electrode. The AgNP GPE was able to detect traces of copper in the tea samples via ASV. The electrode with 80µL mineral oil and 2mg AgNP was chosen as the best electrode and was used to generate the calibration curves for Pb^{2+}, Cd^{2+}, and Cu^{2+}. It was also used in real sample analysis. The concentrations of Cd^{2+} and Cu^{2+} obtained from ASV and AAS have a small percentage difference which depicts the integrity of the fabricated electrode in terms of accuracy. With these characteristics of accuracy and low LOD, as it can detect trace heavy metals in the parts per billion range, the cost-effective heavy metal detection method of anodic stripping voltammetry using the fabricated improvised AgNP-modified GPE favorable with high integrity.

References

1. M. Jaishankar, T. Tseten, N. Anbalagan, B.B. Mathew and K.N. Beeregowda, *Interdiscip. Toxicol.*, 7 (2014) 60.
2. M. Cabral, A. Toure, G. Garçon, C. Diop, S. Bouhsina, D. Dewaele, F. Cazier, D. Courcot, A. Tall-Dia, P. Shirali, A. Diouf, M. Fall and A. Verdin, *Environ. Pollut.*, 206 (2015) 247.
3. R. Nazir, M. Khan, M. Masab, H. Rehman, N. Rauf, S. Shahab, N. Ameer, M. Sajed, M. Ullah, M. Rafeeq and Z. Shaheen, *J. Pharm. Sci. Res.*, 7 (2015) 89.
4. L. Zhu, L. Xu, B. Huang, N. Jia, L. Tan and S. Yao, *Electrochim. Acta*, 115 (2013) 471.
5. S. Palisoc, M. Natividad, N. Martinez, R. Ramos and K. Kaw, *e-Polymers*, 16 (2015)117.
6. S. Palisoc, M. Natividad, P. DeVera and B. Tuason. *Philipp. Sci. Lett.*, 7 (2014) 372.
7. S. Palisoc, M. Natividad, P. DeVera and B. Tuason. *J. New Mat. Electr. Sys.*, 17 (2014) 205.
8. S. Palisoc, M. Natividad, D. Calde and E. Rosopa. *J. New Mat. Electr. Sys.*, 19 (2016) 223.
9. S. Palisoc, N. Valeza, M. Natividad. *Int. J. Electrochem. Sci.*, 12 (2017) 3859.
10. S. Palisoc, N. Causing and M. Natividad, *Anal. Methods*, 9 (2017) 4217.
11. S. Palisoc, K. Kaw, M. Natividad and J. Robles, *J. New Mat. Electr. Sys.*, 20 (2017) 077.
12. S. Palisoc, M. Natividad and C.E.A.Tan, *J. New Mat. Electr. Sys.*, 20 (2017) 089.
13. W. Wonsawat, S. Chuanuwatanakul, W. Dungchai, E. Punrat, S. Motomizu and O. Chailapakul, *Talanta*, 100 (2012) 282.
14. S. Karastogianni and S. Girousi, *Anal. Chem. Insights*, 11 (2016) 1.

15. C. Apetrei, M.L. Rodríguez-Méndez, V. Parra, F. Gutierrez and J.A. De Saja, *Sens. Actuators B Chem.*, 103 (2004) 145.
16. I. Svancara, K. Vytras, J. Barek and J. Zima, *Crit. Rev. Anal. Chem.*, 31 (2001) 311.
17. M.L. Rodríguez-Méndez, M. Gay, C. Apetrei and J.A. De Saja, *Electrochim. Acta*, 54 (2009) 7033.
18. J.C. Ruiz-Morales, J. Canales-Vázquez, D. Marrero-López, S.N. Savvin, P. Núnez, A.J. Dos Santos-García, C. Sánchez-Bautista and J. Peña-Martínez, *Carbon*, 48 (2010) 3964.
19. C.B. Jacobs, M.J. Peairs and B.J. Venton, *Anal. Chim. Acta*, 662 (2010) 105.
20. N. Ikhsan, P. Rameshkumar and N. Huang, *Electrochim. Acta*, 192 (2016) 392.
21. T. Kuwana and W. G. French, *Anal. Chem.*, 36 (1964) 241.
22. F. A. Schultz and T. Kuwana, *J. Electroanal. Chem.*, 10 (1965) 95.
23. G. T.Cheek and R. F. Nelson, *Anal. Lett. A*, 11 (1978) 393.
24. T. Yao and S. Musha, *Anal. Chim. Acta*, 110 (1979) 203.
25. K. Ravichandran and R. P. Baldwin, *J. Electroanal. Chem.*, 126 (1981) 293.
26. K. Kalcher, *Electroanalysis*, 2 (1990) 419.
27. K. Vytras, I. Svancara and R. Metelka, *J. Serb. Chem. Soc.*, 74 (2009)1021.
28. M. H. Parvin, *Electrochem. Commun.*, 13 (2011) 366.
29. T. Mikysek, K. Rosecká, M. Stočes, K. Kalcher and I. Švancara, *Sensing in Electroanalysis*, 8 (2013/2014) 133.
30. M. Pumera, A. Escarpa, *Des. Appl. Electrophor*., 30 (2009), 3315.
31. V. Bansal, V. Li, A. O'Mullane and S. Bhargava, *Cryst. Eng. Comm.*, 12 (2010) 4280.
32. A. J. Marenco, D. B. Pedersen, S. Wang, M. W. P.Petryk and H.-B. Kraatz, *Analyst*, 134 (2009) 2021.
33. Y. Bonfil, M. Brand and E. Kirowa-Eisner, *Electroanalysis*, 15 (2003) 1369.
34. C. Tan, F. Wang, J. Liu, Y. Zhao, J. Wang, L. Zhang, K. C. Park and M. Endo, *Mater. Lett.*, 63 (2009) 969.
35. G.-W. Yang, G.-Y. Gao, C. Wang, C.-L. Xu and H.-L. Li, *Carbon*, 46 (2008) 747.
36. C. M. Welch, C. E. Banks, A. O. Simm, R. G. Compton, *Anal. and Bioanal. Chem.*, 382 (2005) 12.
37. J. Zhuang, L. Zhang, W. Lu, D. Shen, R. Zhu and D. Pan, *Int. J. Electrochem. Sci*., 6 (2011) 4690.
38. K. Wu, H. Lo, J. Wang, S. Yu and B. Yan, *Mater. Express*, 7 (2017) 15.
39. S. Palisoc, D. J. Uy, M. Natividad and T.B. Lopez, *Mater. Express*, 4 (2017) 1.
40. D.S. Rajawat, N. Kumar and S.P. Satsangee, *Journal of Analytical Science and Technology*, 5 (2014) 19.